TESCE ,Vol.29,No.2 pp. 30-48

High Temperature Oxidation of TiAl alloys at low Oxygen Partial Pressure

Wafaa A. Ghanem and Fathy M. Bayoumi

(Central Metallurgical Research and Development Institute)

Abstract

The high temperature oxidation behavior of some TiAl alloys at low partial pressure oxygen (10.1 pascal) at 750^{0}C, 850^{0}C and 950^{0}C. Oxidation mass gain of the alloys at different temperatures was measured and the corroded surface was characterized using SEM, EPMA and XRD. Parabolic oxidation kinetics was observed in most samples suggesting a diffusion limited mechanism followed , generally by a transition in oxidation kinetics to a slower rate. The sample that contains 2.5 % Nb showed least oxidation rate at all temperature. For the other samples, the higher the % of α_2 phase the greater the oxidation rate at 750^{0}C but at 950^{0}C the sample with high % of α_2 is the least in oxidation rate.

Keywords: High temperature – oxidation – heat treatment - TiAl alloys – mass gain – oxygen low partial pressure.

Introduction

Intermetallics specially such as TiAl systems have recently attracted the attention of many researchers[1-5] . TiAl alloys are regarded as very promising candidates for high temperature structural materials because of their low density and high strength at high temperature. However , their tendency for oxidation in air and their reduced ductility at room temperature restrict their application to the high

temperature structure components. Their temperature limit for high temperature oxidation is lower than that for high temperature mechanical properties. This has become an important obstacle for these materials[1,2]. In general, a protective Al_2O_3 scale doesn't form on TiAl, particularly in air, but a scale composed of TiO_2 and Al_2O_3 forms. Such scales grow mostly parabolically with time[3-5]and consists of two or even three layers. Generally, an outer layer of finely dispersed mixture of TiO_2 and Al_2O_3 [3,4,6-8, 9] is observed.

The phase diagram of the TiAl system[10] reveals that there are two main phases can be formed in this alloy. γ phase and α_2 phase. Ti-49Al has a duplex structure ($\gamma + \alpha_2$) while Ti-51Al is a single γ phase. Several attempts were made to develop better oxidation resistance of this alloy for example the addition of alloying elements such as molybdenum, silicon, phosphorous or niobium[11-14] . Other methods such as heat treatment, spray coating and plasma coating have been developed[15-17] . Thermodynamics predict that the tendency to oxidize aluminum rather than titanium is increased as the partial pressure of oxygen decrease. The aim of this work is to study the high temperature oxidation behavior of some TiAl alloys at low oxygen partial pressure (10.1 pascal). This may lead to develop and understand a technique for preoxidation to create a protective film and hence protect the alloy from high temperature oxidation.

Experimental

Materials

The Ti-Al alloys used in this investigation were kindly provided by Kobe Steel Co. Japan. The details of the heat treatment of the alloys were introduced in a previous work[18] . Table 1 lists the chemical composition and the % of α_2 phase content in the alloys used.

Table 1 The alloys used and the contents of α_2 phase in a matrix of γ phase

Alloy	α_2 phase
Ti-51 Al	0 %
Ti-51 Al	15 %
Ti-49 Al	25 %
Ti-51 Al	37 %

Fig. 1 shows a schematic representation of the system used for measuring the mass gain for the samples oxidized in a reduced oxygen partial pressure, 10.1 pascal. Pure helium and oxygen, passed over silica gel (1) for drying, then passed through flowmeters (2) to adjust the volume proportions that the oxygen is 100 ppm then the gases are mixed through mixing chamber (3). Samples were taken from the mixing chamber and analyzed to ensure the proper proportions (100 ppm oxygen). The gas mixture is passed through the furnace (4). The electric furnace (4) is regulated by Heraus temperature regulator and Pt/Pt-Rh thermocouple. When the temperature reaches the corresponding value, the gas mixture is allowed to pass, after about 2 minutes the sample is placed at the hot zone using the holder (5), through the window (6), which is closed tightly after placing the sample. The effluent gas mixture is taken away through the exit (7) to purify the helium for recycling. The corroded surfaces of the samples were analyzed using X-ray diffraction analysis using a Shimadzu XRD 610 diffractometer, from Shimadzu (Japan). The instrument uses a Cu tube producing Cu K_{α_1} radiation at 600 W with a wavelength of λ = 1.54 Å. X-ray microanalysis (XMA) using Shimadsu instrument were used. The morphology of the corroded surface was examined using an SEM model JEOL-JSM.T20, Japan.

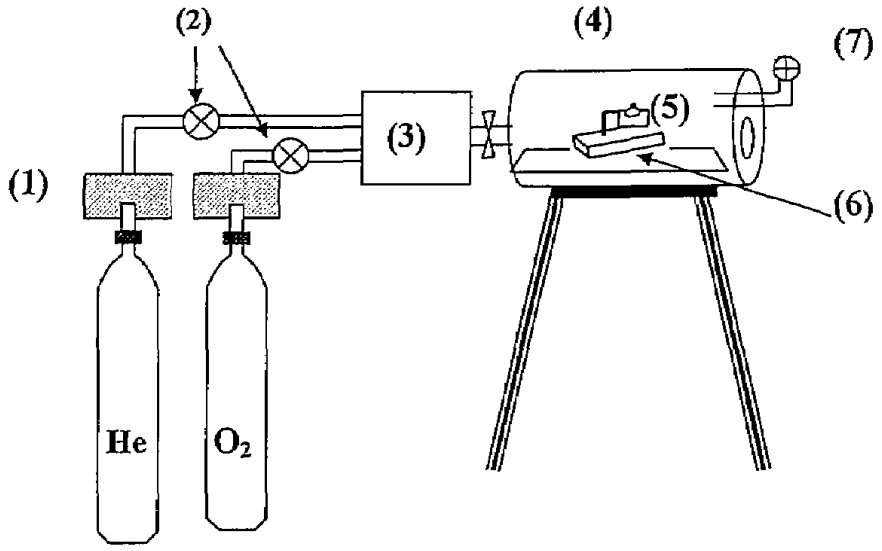

Fig. 1 Schematic representation for the system used for high temperature oxidation of Ti-Al alloys in reduced oxygen partial pressure (10.1 Pascal) mixed with helium gas.

Results and Discussions

Fig.2 shows the variation, with time, of the mass gain of the alloys oxidized at 10.1pascal oxygen at 750^0C. Generally, in the first part of the curve, region (I) the kinetics reveals parabolic behavior

$\{d \ln (\text{mass gain})\} / d \ln t \approx 0.5$ (1)

This reveals diffusional limited kinetics and suggests that the formed oxide, progressively, acts as barrier to retard the inward diffusion of oxygen and/or the outward diffusion of the metal ions.

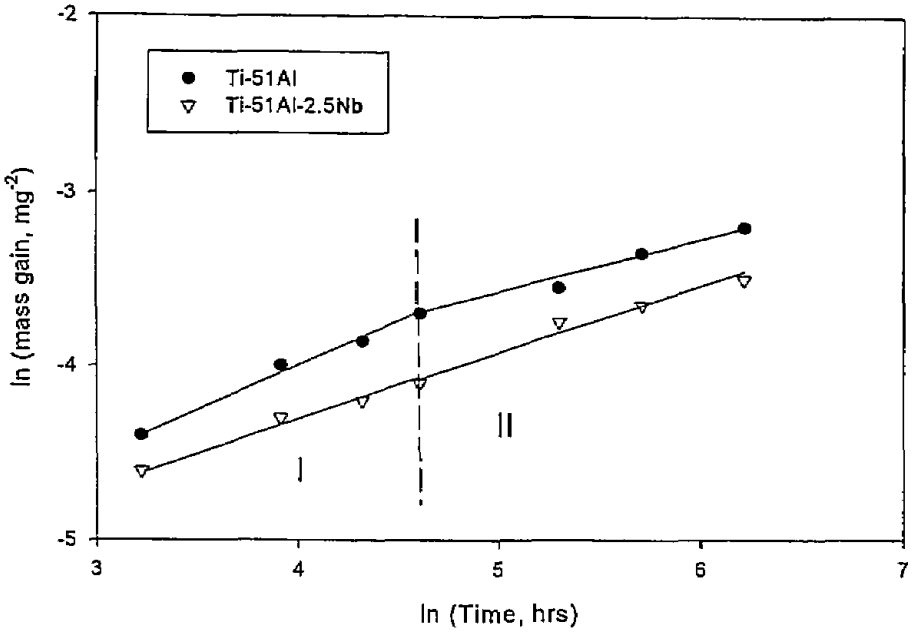

Fig.2 Variation with the time of oxidation of the mass gain of the alloy Ti-51Al with and without addition of 2.5% Nb at low partial pressure oxygen (10.1 pascal) at 750^{0}C

According to thermodynamics, the driving force for oxidizing aluminum compared to titanium increase by decreasing the partial pressure for oxygen, this can be shown as follows, for reaction of oxidation of a metal M ;

$$xM + \frac{y}{2}O_2 \rightarrow M_xO_y \qquad (2)$$

$$\Delta G^0 = -RT\ln\left[\frac{a_{prod}}{a_{react}}\right] \approx +\frac{y}{2}RT\ln p_{O_2} \qquad (3)$$

Applying the above equation for the oxidation of aluminium in air and in 10.1 pascal oxygen/ helium

$$2Al + \frac{3}{2}O_2 \rightarrow Al_2O_3 \qquad (4)$$

then

$$\Delta G^0 = \frac{3}{2}RT\ln P_{O_2} \qquad (5)$$

for oxidation of titanium

$$Ti + O_2 \rightarrow TiO_2 \qquad (6)$$

$$\Delta G^0 = RT \ln P_{O_2} \qquad (7)$$

The lower in free energy as the partial pressure decrease in case of oxidation of aluminium is greater than in case of oxidation of titanium. This means the expecting predominance of Al_2O_3 at lower oxygen partial pressure.

However the alloy that contains 2.5 % niobium shows lower oxidation rate. This may be attributed to the argument that niobium fills the electron deficient vacancies in the n-type oxide TiO_2 or Al_2O_3 (or both). Consequently retard the inward diffusion of oxygen and to a lower oxidation rate.

Fig.3 shows the time variation of the mass gain for the alloys with different % of α_2 phase in 10.1 Pascal oxygen at 750^0C. It can be noticed that the sample with no α_2 phase is the best as oxidation resistance under these conditions, and generally the oxidation rate increase by increasing the % of α_2 phase. The general trend in the kineticsis the parabolic behavior at the first part of the curve followed by a slower rate region:

$\{d \ln (\text{mass gain})\} / d \ln t \approx 0.5$ for region 1

$\{d \ln (\text{mass gain})\} / d \ln t \approx 0.3 - 0.4$ for region 2

However, the oxidation rate constant increases by increasing α_2 content in the alloy. This is compatible with our previous findings for the oxidation in air and others findings [18-20]. This was explained in terms of the scavenging effect of the α_2 phase for oxygen. Although the partial pressure of oxygen here is small, the same phenomena is observed.

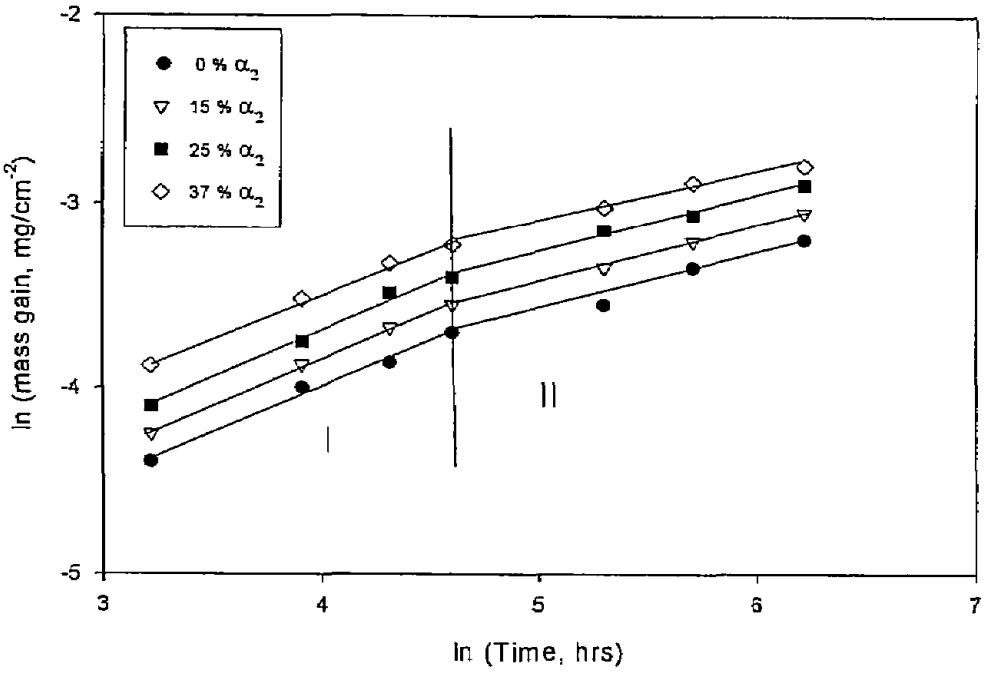

Fig.3 Variation with the time of oxidation of the mass gain of the alloy Ti-51Al with different contents of α_2 phase at low partial pressure oxygen (10.1 pascal) at 750^{0}C

Fig. 4 is the time variation of the oxidation mass gain in 10.1 Pascal oxygen at 850^{0}C. The curves , in general can be classified into two regions for both alloys. First region is almost parabolic behavior and during the second region the oxidation slows down. The sample with 2.5% Nb, in region I is exactly parabolic which reveals that the oxidation process is mainly controlled by diffusion. The oxidation rate constant increased by increasing the temperature in both samples under the test conditions.

The general trend of the parabolic behavior which eventually followed by slower rate of the oxide growth is also observed for the oxidation of the alloys with different contents of α_2 phase in 10.1 pascal oxygen at 850^{0}C, Fig 5 . However, the order, now, doesn't fit the order of increasing α_2 phase content. The sample with 37%

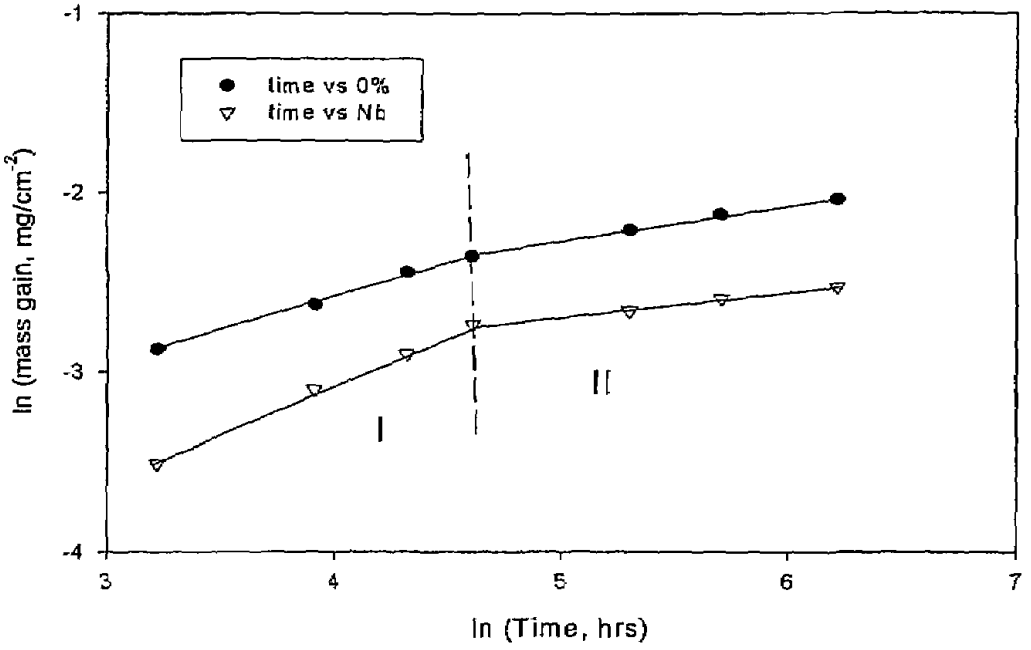

Fig.4 Variation with the time of oxidation of the mass gain of the alloy Ti-51Al with and without addition of 2.5% Nb at low partial pressure oxygen (10.1 pascal) at 850^{0}C

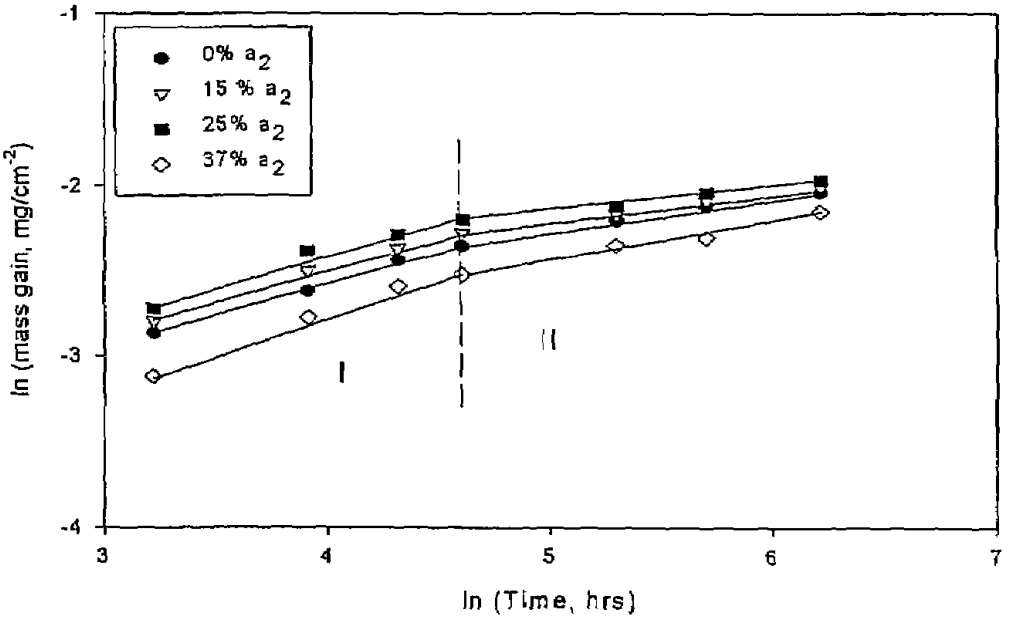

Fig.5 Variation with the time of oxidation of the mass gain of the alloy Ti-51Al with different contents of α_2 phase at low partial pressure oxygen (10.1 pascal) at 850^{0}C

α_2 phase is now has the slowest rate of oxide growth. The order of the other samples is 0% > 15 % > 25% α_2 phase.

At the highest temperature of the test, 950^{0}C , Fig. 6, here the parabolic behavior has been followed by, almost leveling off of the curve. This lead us to expect that, generally a change in mechanism occurs and a transition from parabolic to a slower rate of oxide growth occurs. The rate of oxide growth in the second region decreases with increasing the temperature. One may conclude that a protective oxide film composed mainly from Al_2O_3 is formed during the oxidation. The crystallinity of this oxide grows better as the temperature increase becoming more protective.

A dramatic change in oxidation behavior can be observed for alloys with different contents of α_2 phase. The order is completely riverside and the rate of oxidation at 950^{0}C , Fig 7, now is reversed. The rate of oxidation of the alloy samples under the test conditions is inversely related to the % of α_2 phase content in the samples. This surprising result can be explained on reference to Fig. 8. Fig. 8 is SEM micrographs for cross section of the corroded sample that contains 37% α_2 phase oxidized in 10.1 Pascal at 950^{0}C for 500 hrs. The micrograph shows that a phase transition occurs from α_2 phase into γ phase both near surface and in the bulk of the alloy. This transformation is due to aging effect due to the temperature of the test. A finding like this was observed in the reference [21].

Fig. 9 is SEM micrographs comparing the oxidation of the alloy Ti-51Al with 37% α_2 phase at 950^{0}C in air (photo (a)) and in 10.1 Pascal oxygen (photo (b)). It can be noticed that sample (b) is covered with fine grains; it is expected to be Al_2O_3. Sample (a) is covered with bigger TiO_2 crystals on its surface. The composition of the film for the sample Ti51Al with 37% α_2 phase was confirmed by XRD that it is

formed mainly from Al_2O_3 and TiO_2 , Fig 10. Fig. 11 and 12 are x-ray image and line spectra for the alloy Ti-51Al containing 37% α_2 phase oxidized in 10.1 Pascal oxygen for 500 hrs. They reveals that the oxide film is composed of an outer Al_2O_3 layer followed by a thin inner layer which is composed of a mixture of Al_2O_3 + TiO_2.

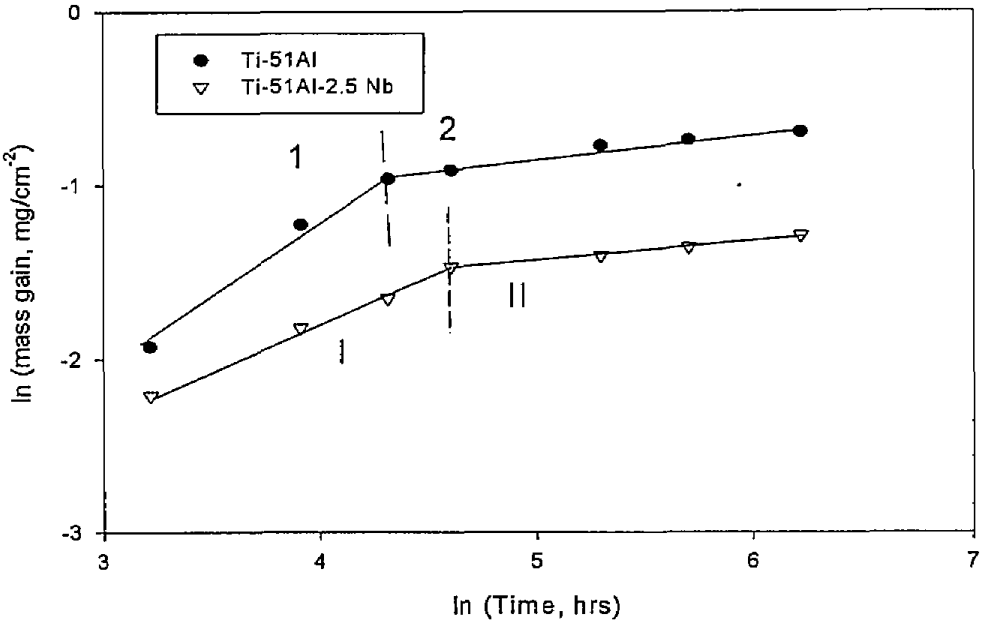

Fig.6 Variation with the time of oxidation of the mass gain of the alloy Ti-51Al with and without addition of 2.5% Nb at low partial pressure oxygen (10.1 pascal) at 950°C

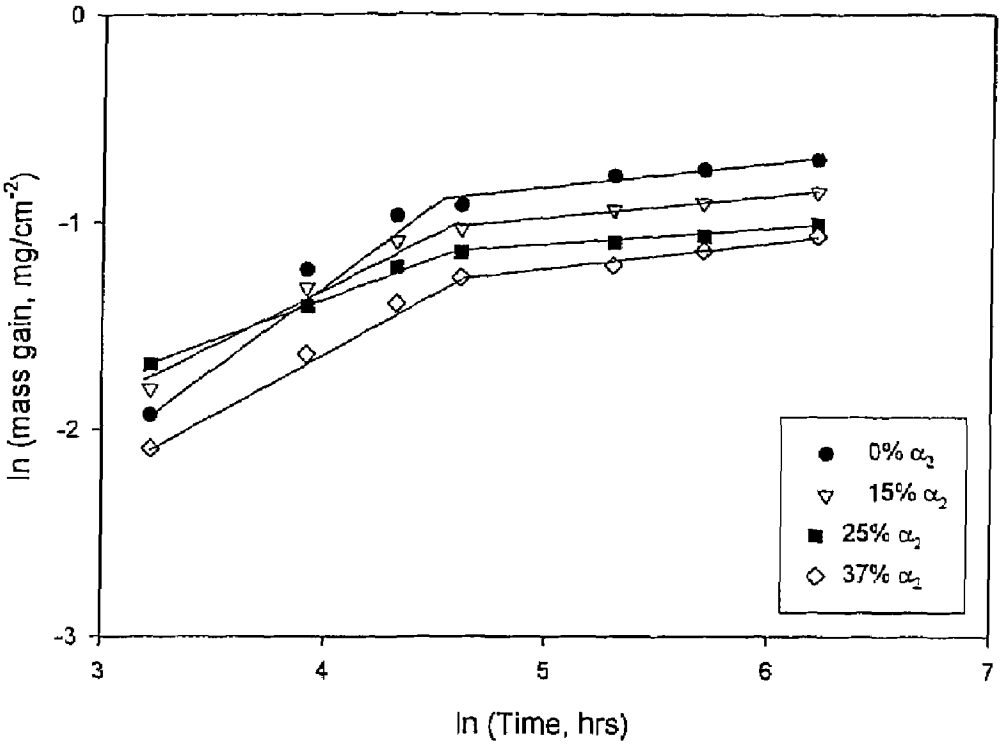

Fig.7 Variation with the time of oxidation of the mass gain of the alloy Ti-51Al with different contents of α_2 phase at low partial pressure oxygen (10.1 pascal) at 950^{0}C

(a) near surface

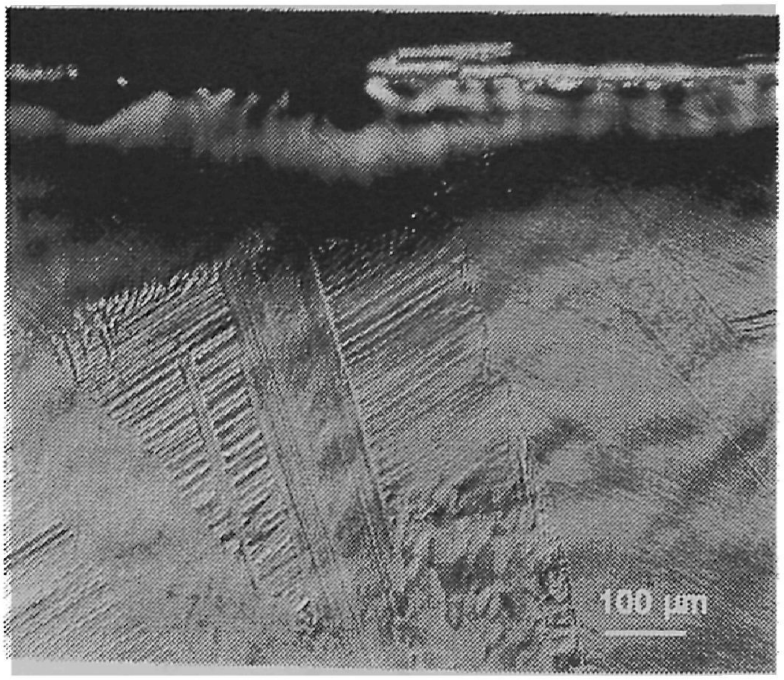

(b) bulk

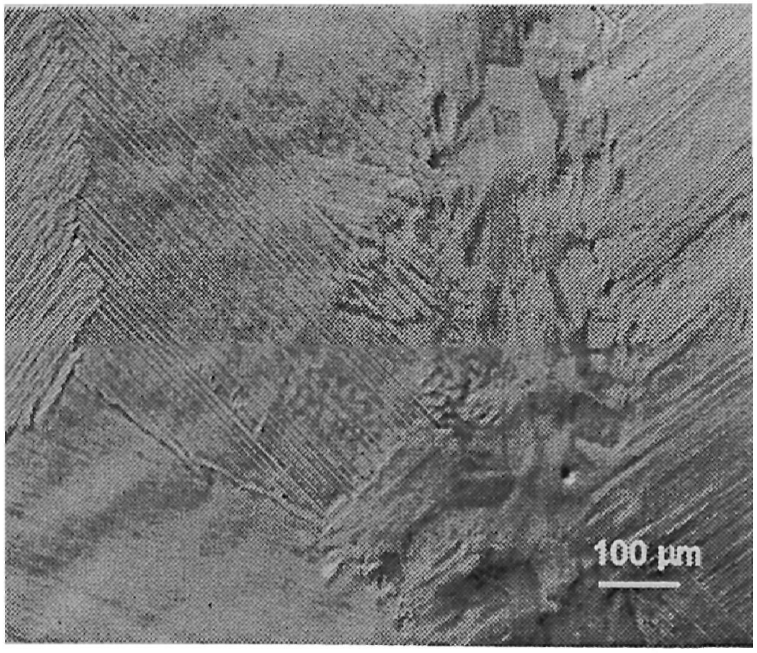

Fig. 8 SEM micrograph for cross section of Ti-51Al alloy with 37% α_2 phase after oxidation in low partial pressure oxygen (10.1 Pascal) at 950^{0}C for 500 hrs, (a) near surface, (b) bulk of the alloy

Low Oxygen (b)

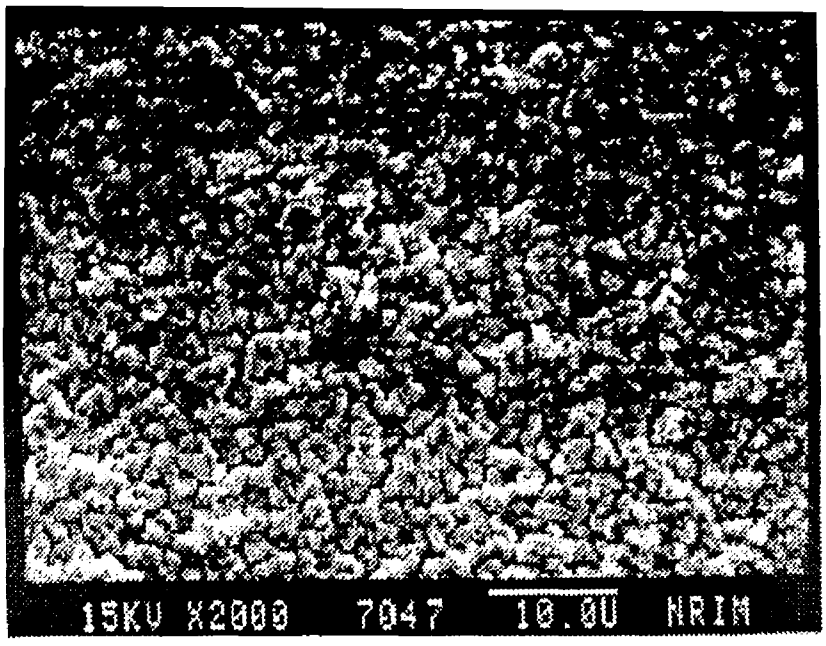

Air (a)

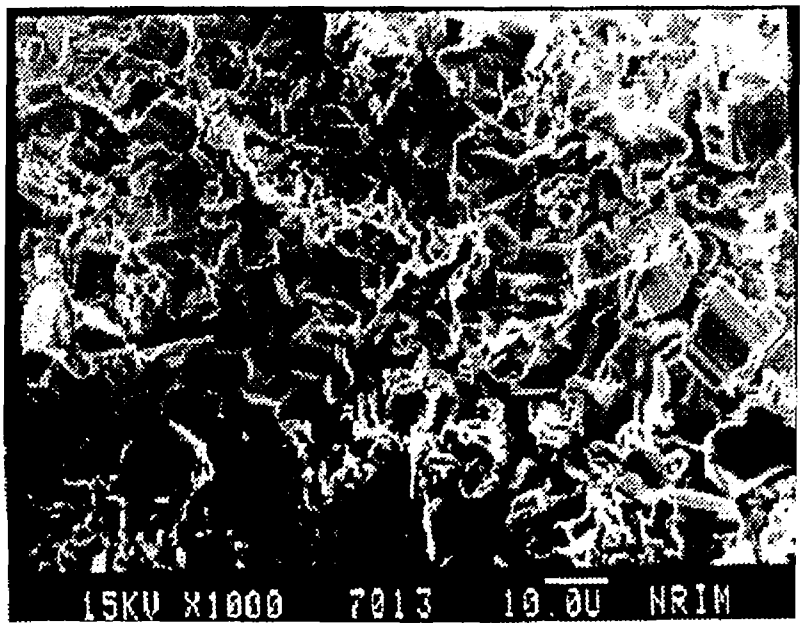

Fig. 9 SEM micrographs for the oxidized surface of Ti-51Al alloy with 37% α_2 phase after oxidation in air and in low partial pressure oxygen (10.1 Pascal) at 950^{0}C for 500 hrs

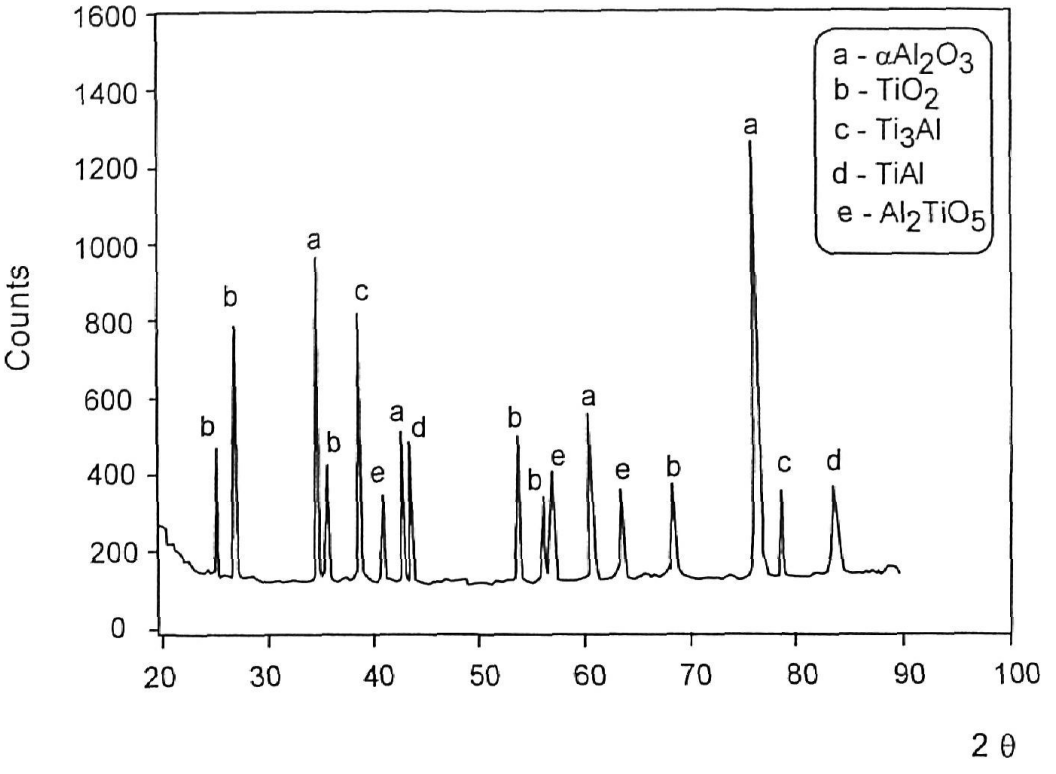

Fig. 10 XRD for Ti-51Al alloy with 37% α_2 phase after oxidation in low partial pressure oxygen (10.1 Pascal) at 950^0C for 500 hrs

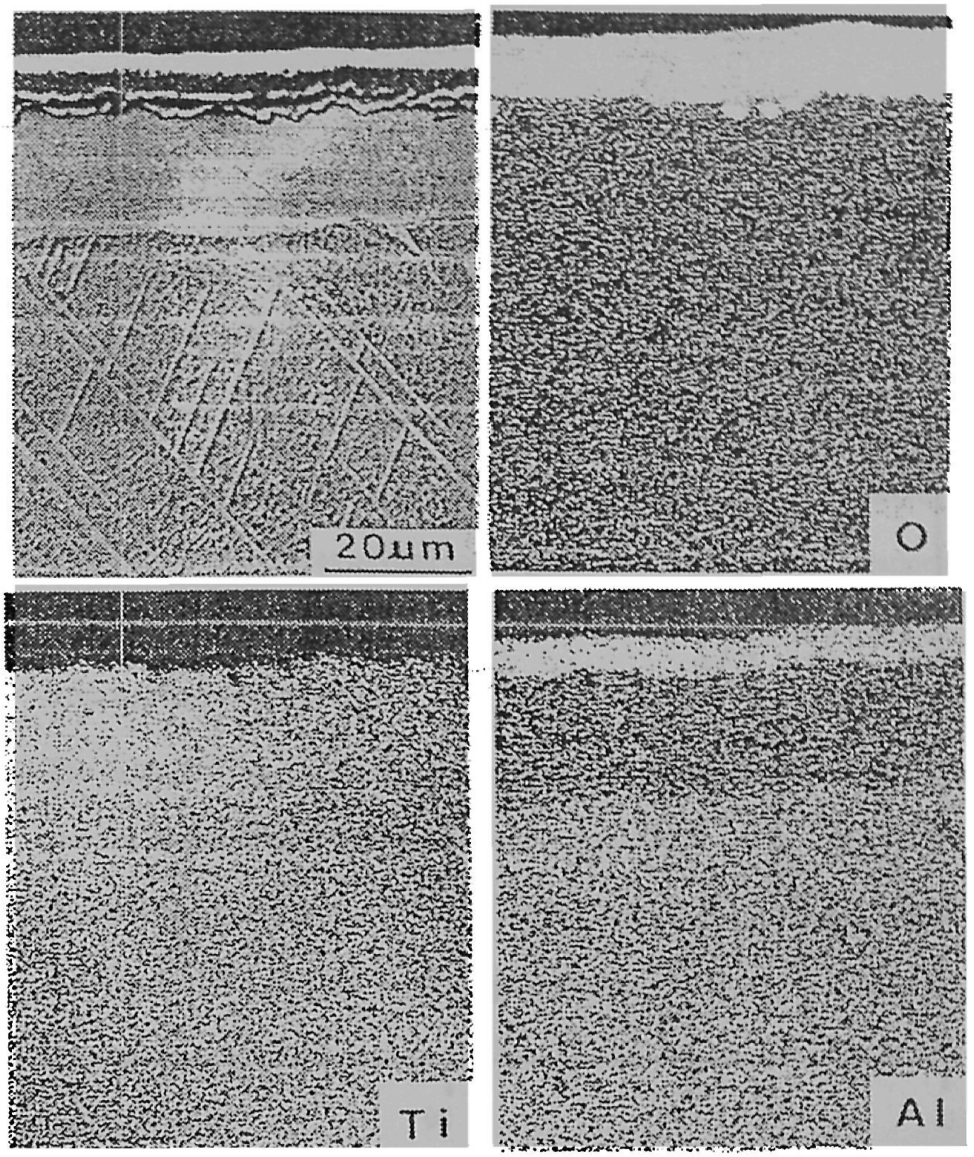

Fig.11 X-ray image for a cross section of Ti-51Al alloy with 37% α_2 phase after oxidation in air and in low partial pressure oxygen (10.1 Pascal) at 950^{0}C for 500 hrs

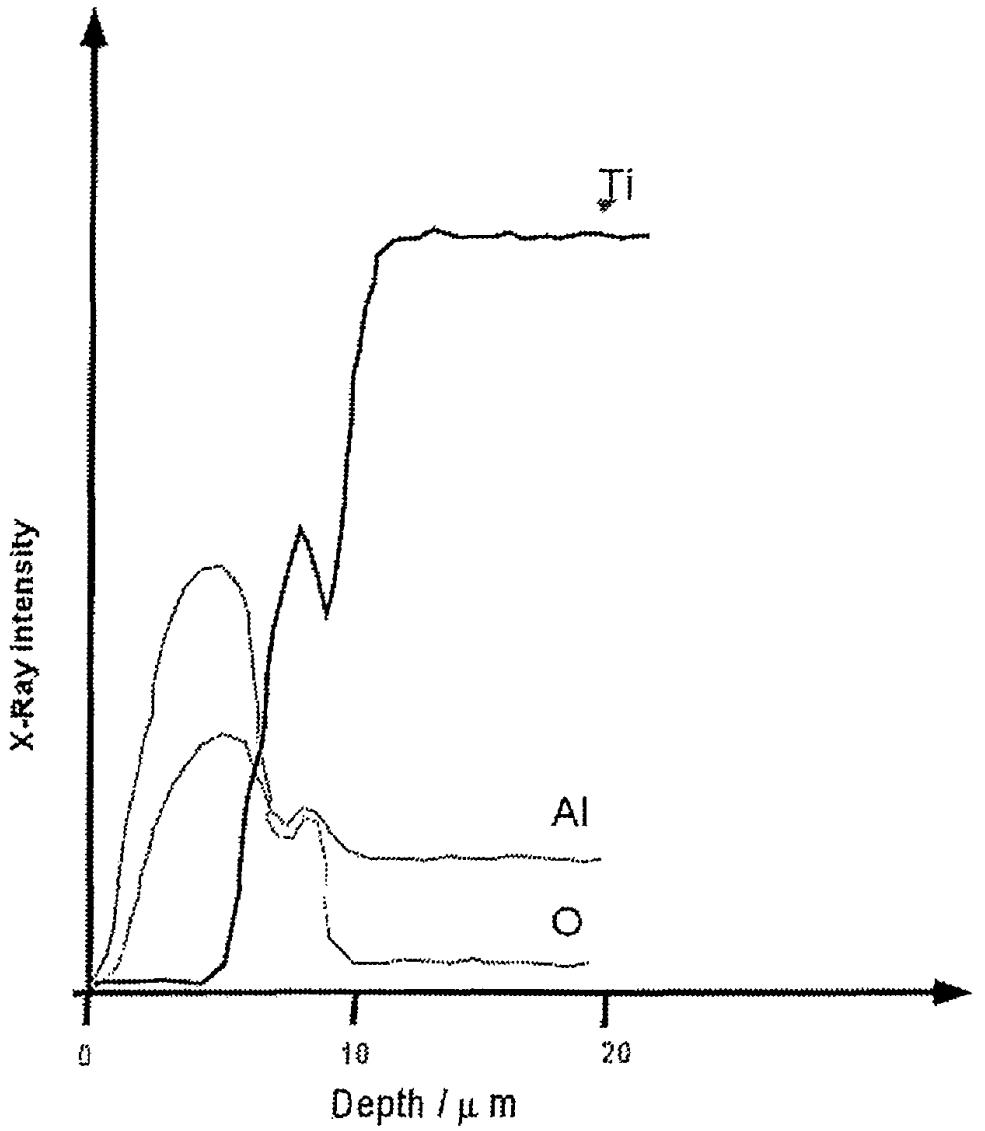

Fig. 12 X-ray line spectra (EPMA) for a cross section of Ti-51Al alloy with 37% α_2 phase after oxidation in air and in low partial pressure oxygen (10.1 Pascal) at 950^{0}C for 500 hrs

Conclusions

1. The kinetics of the oxidation at low partial pressure reveals it is two stages the first is parabolic and the second is a low oxidation rate stage.
2. The gradient of the second stage oxidation decrease by temperature, the oxide film becomes stable and protective
3. Presence of α_2 phase increase the oxidation rate at the lower temperature (750^0C) due to acting as oxygen scavenger but lower the rate of oxidation at the higher temperature due to ageing effect which results in transformation from α_2 phase into γ phase.
4. The oxide film on Ti-51Al alloys is formed mainly from Al_2O_3 on the surface and thin a thin layer of the mixed oxides $Al_2O_3 + TiO_2$.
5. A promising tool to protect TiAl alloys for oxidation at high temperature is to make pre-oxidation at low oxygen partial pressure to enhance formation of protective Al_2O_3 layer.

Acknowledgment

The authors express their thanks and gratitude to the stall members in National Research Institute of Metals (NRIM), Japan for providing facilities for several measurements and valuable discussions specially Prof. Dr. Tanabe. Greatest thanks also are to Dr. B. G. Ateya for valuable discussions

References

1. M. Takeyama, Mater. Sci. and Engn., A152, 269 (1992)
2. S.C. Huang, Structural Intermetallics. In: R. Darolia et al., editors. Warrendale, PA: The Minerals, Metals and Materials Society, 299-307 (1993).

3. S. Becker, A. Rahmel, M. Schorr and M. Schütze, Oxid. Met., 38, 425 (1992).
4. G. H. Meier, D Appalonia, R. A. Perkins and K. T. Chiang, In: T. Grobstein and J. Doychak, editors. Oxidation of High Temperature Intermetallics, Warrendale, PA, USA: TMS, p. 185. (1988)
5. E. U. Lee and H. Waldman, Scripta Metall. 22, 1389 (1988)
6. K. Kasahara, K. Hashimoto, H. Doi, and T. Tsujimoto, J. Jpn. Inst. Met. 53, 58 (1989).
7. N. S. Choudhury, H. G. Graham, and J. W. Hinze, in Properties of High Temperature Alloys with Emphasis on Environmental Effects, Z. A. Foroulis and F. S. Pettit, eds., The Electrochemical Society, Princeton, p. 668 (1976).
8. E. Kobayashi, M. Yoshihara, and R. Tanaka, High Temp. Technol. 8, 179 (1990).
9. Wafaa A. Ghanem and Fathy M. Bayoumi, Al-Azhar Bulletin of Science, in press
10. Binary Alloy Phase Diagrams, T. B. Massalski ed., ASM, (1986).
11. R. A. Perkins, K. T. Chiang, and G. H. Meier, Scripta Metall. 21, 1505 (1987)
12. T.T. Cheng, M. R. Willis and I. P. Jones, Intermetallics, 7, pp.89-99 (1999)
13. Y. Norio, K. Takuro, Y. Takayuki and O. Osamu, Mater. Trans. V 43, pp. 3211-3216 (2002)
14. A. Donchev, B. Gleeson and M. Schutze, Intermetallics, v 11, n 5,pp. 387-398 (2003).
15. H. Anada and Y. Shida, J. Jpn. Inst. Metals, 58, pp. 746-753 (1994).
16. W.Fang, H. S. Ko, H. Hashimoto, T. Abe and H. Y. Park, Mater. Sci. and Eng. A. v 329-331, pp. 708-712 (2002).

17. M. Yoshihara, S. Taniguchi and C. Y. Zhu, Mater. Sci. Forum, v 369-372, pp. 395-402 (2001)

18. Wfaa A. Ghanem and Fathy M. Bayoumi, Under publication

19. T. Kumagai, E. Abe, T. Kimura and M. Nakamura, Scripta Materialia, vol. 34, No. 2, pp. 235-242, 1996.

20. T. Kumagai, E. Abe, M. Takeyama and M. Nakamura, Mat. Res. Soc. Symp. Proc. 364, 181 (1995).

21. I. Mutoh, K. Homma, T. Tanabe and M. Nakamura, J. Nuclear Mater. 231 p. 132-140 (1996).